Supplement of Atmos. Chem. Phys., 24, 4083–4104, 2024
https://doi.org/10.5194/acp-24-4083-2024-supplement

Atmospheric Chemistry and Physics
Open Access
EGU

Supplement of

Sharp increase in Saharan dust intrusions over the western Euro-Mediterranean in February–March 2020–2022 and associated atmospheric circulation

Emilio Cuevas-Agulló et al.

Correspondence to: Emilio Cuevas-Agulló (emilio.cuevas@uva.es) and Sara Basart (sbasart@wmo.int)

S1. Strong Dust Intrusions in Western Euro-Mediterranean (WEM) in winters 2020-2022

In this section we have collected the links to the web news pages and technical report previews dealing with strong dust events impacted the WEM in February-March 2020-2022 (Table S1). These dust events merited preliminary and widely disseminated analysis by international institutions such as the World Meteorological Organisation (WMO), the European Organisation for the Exploitation of Meteorological Satellites (EUMETSAT), the Copernicus Atmosphere Monitoring Service (CAMS), and/or Barcelona Supercomputing Center (BSC). The media had the opportunity to show shocking images, such as the dramatic reduction in visibility in some cities in southern Europe and of people skiing on reddish-coloured snow in the Pyrenees and the Alps because of dust deposition. These dust events caused great social alarm, being associated, in much news, with the current climate change scenario.

Table S1: Links to web news and technical report previews on strong wintertime dust intrusions over Western Europe in the 2020-2022 period (last access to all links on 12 February 2024).

Dust event	Entity issuing the news and source
Feb 2020	EUMETSAT: https://user.eumetsat.int/resources/case-studies/dust-over-the-canaries WMO: https://library.wmo.int/records/item/57466-no-4-may-2020
Feb 2021	Copernicus: https://atmosphere.copernicus.eu/saharan-dust-colours-skies-and-snow Copernicus: https://atmosphere.copernicus.eu/2021-review-cams-goes-strength-strength EUMETSAT: https://user.eumetsat.int/resources/case-studies/dust-over-south-eastern-europe EUMETSAT: https://vuser.eumetsat.int/resources/case-studies/meteosat-11-captures-plume-of-saharan-dust WMO: https://wmo.int/media/news/sand-and-dust-storm-hits-europe WMO, Airborne Dust Bulletin 2021: https://www.imgw.pl/sites/default/files/2021-07/wmo_airborne_dust_bulletin_5_en.pdf BSC: https://www.bsc.es/news/bsc-news/exceptional-february-europe-terms-saharan-dust-intrusion-episodes
Mar 2022	Copernicus: https://atmosphere.copernicus.eu/historical-saharan-dust-episode-western-europe-cams-predictions-accurate Copernicus: https://policy.atmosphere.copernicus.eu/reports/pdf/CAMS2-71_D3.2.1-2022-1_PM10_episode_13-18March2022_v1.pdf EUMETSAT: https://view.eumetsat.int/productviewer?v=18705 EUMETSAT: https://alarm-project.eu/2022/03/21/detecting-dust-and-ash-to-provide-key-information-to-aviation-stakeholders/ ICARO: https://www.icare.univ-lille.fr/saharan-dust-gushes-over-europe-march-15-2022

S2. Unveiling AOD Anomalies for Wintertime Dust Events (2003-2019 vs. 2020-2022)

MODIS aerosol optical depth at 550nm (AOD) product (see Section 2.1) is the reference dataset used for the identification of the dust episodes for the period 2003-2012. The difference of the MODIS AOD distributions between the two dust periods (2003-2019 and 2020-2022) is highly significant (p-value $<<0.01$, as inferred from a Wilcoxon rank sum test), supporting the choice of the anomalous period (Figure S1).

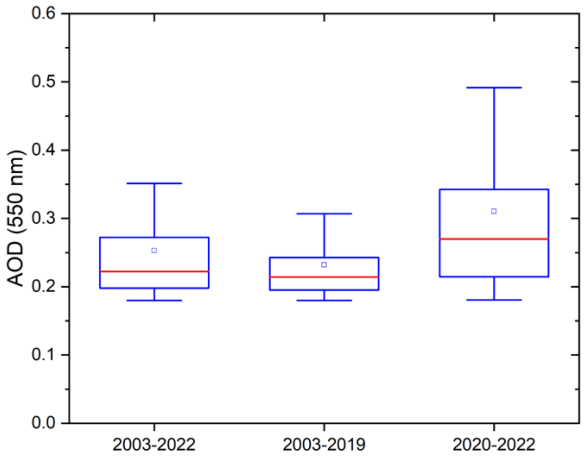

Figure S1: Boxplots of daily AOD for three periods: 2003-2022, 2003-2019 and 2020-2022. Lower and upper boundaries for each box are the 25th and 75th percentiles, the red line is the median value, the blue dots are the mean values, and hyphens indicate the maximum and minimum values. Results are based on MODIS AOD database.

To ensure that MODIS can be considered as representative database for the purpose of the present analysis, in terms of spatio-temporal distribution and intensity, MODIS is compared with ground-observations from the global AERONET network (Section S2.1) and an aerosol reanalysis based on MERRA-2 (Section S2.2).

S2.1. AOD MODIS-AERONET comparison

To ensure that MODIS is also a representative dataset in terms of magnitude of dust events, we compare MODIS and AERONET collocated points. Aerosol Robotic Network (AERONET, Holben et al., 1998; Giles et al, 2019), is a global network of ground-based sun photometers that measure atmospheric aerosols. These instruments provide valuable data for studying air quality, climate, and environmental changes. AERONET direct-sun Version 3 cloud-screened AOD (at 500 nm, i.e. the closest wavelength available to the reference 550 nm) data (Giles et al., 2019) is compared with MODIS AOD data. We have used daily AERONET AOD data of five stations within our study region (El Arenosillo, Palma de Mallorca and Palencia in Spain, Evora in Portugal, and Toulouse MF in France) to evaluate daily MODIS AOD data (Figure S2). For the comparison, the closest MODIS pixel to the AERONET station is used. The results show a good correlation between Évora and Palencia AERONET and MODIS AOD with values of bias ≈ 0.001-0.002 and Pearson coefficient (R) >0.6. For Arenosillo, Palma de Mallorca, and Toulouse, R is ≈ 0.4 (Table S2).

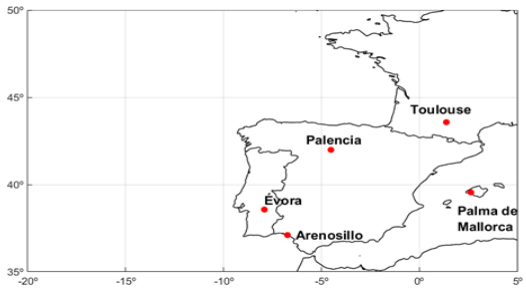

Figure S2: Location of the AERONET stations used in this study.

Table S2: Statistics for the bias (MODIS AOD - AERONET AOD) and Pearson coefficient (R) between MODIS and AERONET AOD for five AERONET stations. Their location is shown in Figure S2.

AERONET Station	Period of data	Bias	Pearson (R) (p-value)
Arenosillo	13/03/2003 – 31/03/2022	-0.080	0.469 (<<0.01)
Évora	15/02/2004 – 27/03/2022	-0.002	0.645 (<<0.01)
Palencia	15/02/2004 – 31/03/2022	+0.001	0.672 (<<0.01)
Palma de Mallorca	26/03/2013 – 28/03/2022	-0.002	0.478 (0.003)
Toulouse MF	10/03/2014 – 31/03/2022	+0.043	0.413 (0.007)

S2.2. AOD MODIS-MERRA-2 reanalysis comparison

Numerical modelling has the advantage of produce spatially and temporally uniform data. While atmospheric-chemistry reanalyses are not error-free, dust reanalysis enables study of dust processes in remote areas, where there are insufficient observational data. A reanalysis product using data assimilation method that combines observational data and model information is undoubtedly a good tool for assessing dust storms and their associated transport at regional and global scales (e.g., Escribano et al. 2022). Because MODIS can provide limited coverage during wintertime because of the presence of clouds, MERRA-2 reanalysis, which provides representative and complete dust fields in space and time, is used to support the results obtained with MODIS about the anomaly of the events identified in 2020-2022 with respect 2003-2019. MERRA-2 uses the GEOS-5 Earth system model (Molod et al., 2015) and the three-dimensional variational data assimilation (3DVar) Gridpoint Statistical Interpolation analysis system (Kleist et al. 2009). The MERRA-2 dataset contains many meteorological and atmospheric composition parameters (including dust). MERRA-2 assimilates aerosol and meteorological observations jointly within GEOS-5. The assimilation of AOD in GEOS-5 includes relationships between MODIS and AVHRR radiances with AERONET calibrated AOD (550 nm), as well as MISR 550-nm AOD over bright surfaces and surface-based AERONET AOD observations at 550 nm (Buchard et al., 2017). MERRA-2 has been specially optimized for aerosols and dust reanalysis.

First, MODIS and MERRA-2 collocated (in space and time) points are compared. In total for 2003-2022, 1796 collocated points are identified. We have calculated the correlation between MODIS and MERRA-2 reanalysis AODs in our study region, resulting in a Pearson correlation coefficient (R) of 0.868, and being 0.774 (mean bias << 0.01) when using only the dust days (see Figure S3).

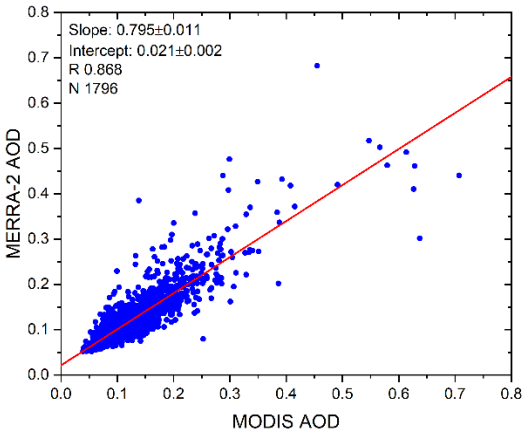

Figure S3: Scatterplot of MERRA-2 versus MODIS AOD between 2003 and 2022 considering only identified dust days in our catalogue. The red solid line is the least-square fit. The least-square fit is show in the legend. R is correlation coefficient Pearson and N is the number of days.

For the assessment of the changes in the meridional transport of Saharan dust, monthly mean values of the MERRA-2 reanalysis Dust column V-wind mass flow (DUPLUXV) variable has been computed for an extended winters (December, January, February, and March) in the two periods of years 2003-2019 and 2020-2022 (Figure S4).

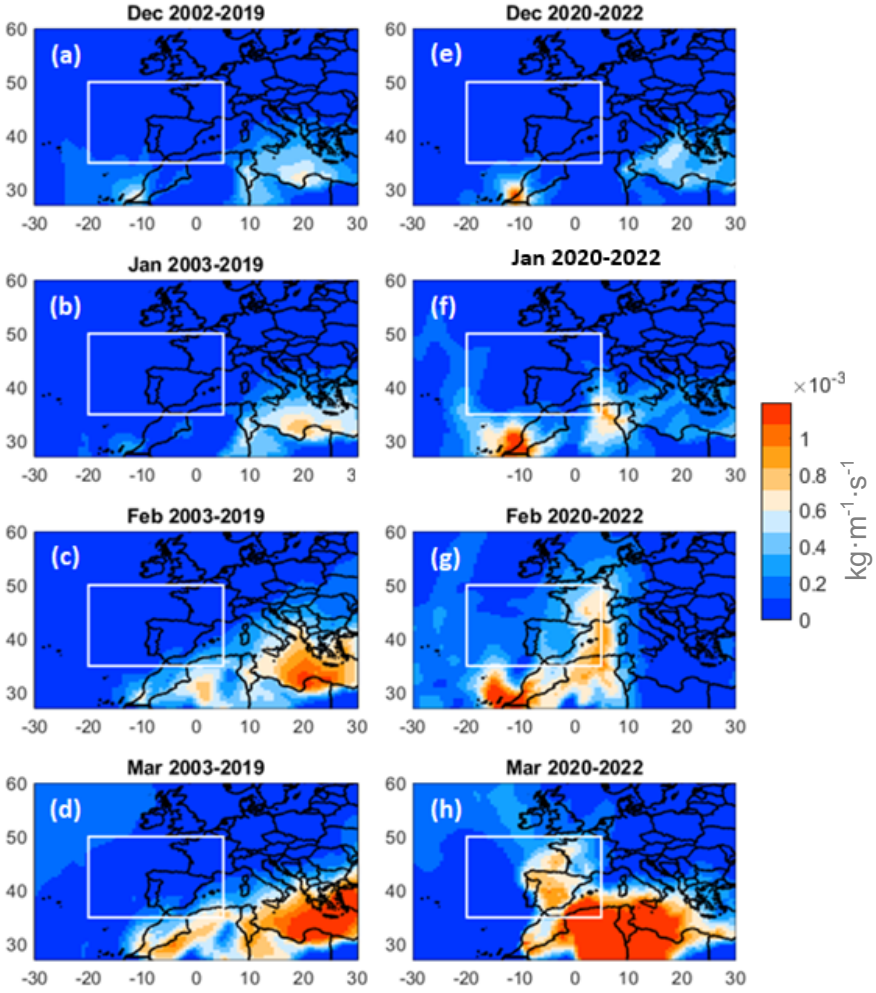

Figure S4: MERRA-2 averaged dust column V-wind mass flux (DUPLUXV; kg m^{-1} s^{-1}) for December, January, February, and March in the 2003-2019 period ((a), (b), (c) and (d)) and 2020-2022 period ((e), (f), (g) and (h)). Rectangle with a white perimeter [35ºN-50ºN, 20ºW-5ºE] marks the study area of dust intrusions over WEM.

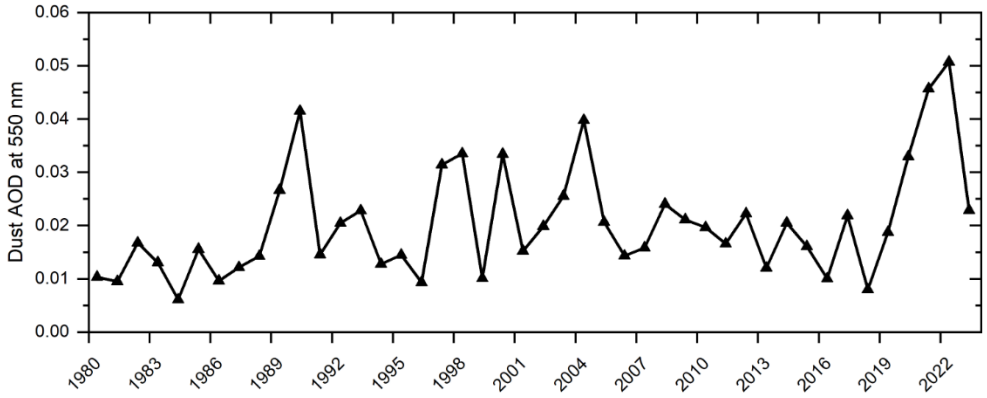

Figure S5: Time series of averaged dust AOD at 550nm from MERRA-2 for February--March (FM) of 1980-2023 over the WEM [35°-50°N, 20°W-5°E] which corresponds to the white perimeter in Figure S4.

The boxplots of Figure S6 show similar MERRA-2 dust-AOD values for both periods, 1980-2002 and 2003-2019. Figure S6 also displays a pronounced increase in dust-AOD between 2020 and 2022, being significantly different from any other reference period considered (p-value <<0.01). These results stress again the degree of exceptionality of February-March 2020-2022, supporting our definition of anomalous dust period.

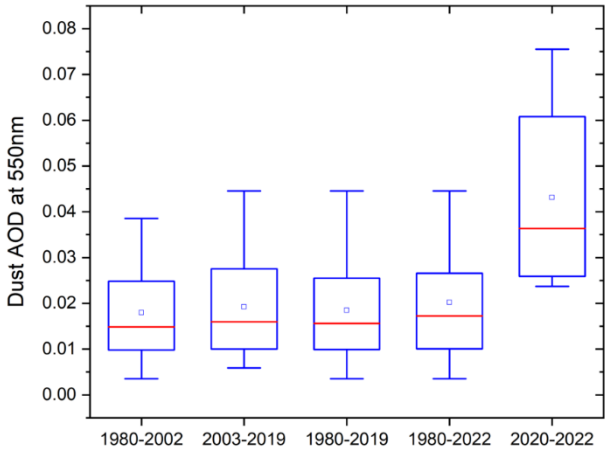

Figure S6: Boxplots of monthly mean MERRA-2 Dust AOD at 550nm over the WEM [35°-50°N, 20°W-5°E] for February - March months of five periods (1980-2002, 2003-2019, 1980-2019, 1980-2022 and 2020-20,22). Lower and upper boundaries for each box are the 25th and 75th percentiles; the red line is the median value; the blue dot is the mean value; and hyphens indicate the maximum and minimum values.

In conclusion, the results of MERRA-2 agree with the ones obtained with MODIS. This confirms the anomalous 2020-2022 vs. 2003-2019 in terms of dust transport over WEM and supports the use of the MODIS dataset for the identification of dust events.

S3. Unraveling the Dust Puzzle: Land factors

The Crop monitoring in Europe Bulletin (Bassu et al., 2022; Ben Aoun et al., 2022) of the Joint Research Center (JRC) Monitoring Agricultural ResourceS (MARS) reported that drought conditions in the Maghreb region have severely impacted yield potential, and even caused crop failure in parts of Morocco in February-March 2022 (see Figure S7). The reduction of vegetation cover in the Maghreb is also confirmed by satellites (see Figure S8). Data corresponding to February and March 2023 is not available by the time that the results of the present analysis were produced.

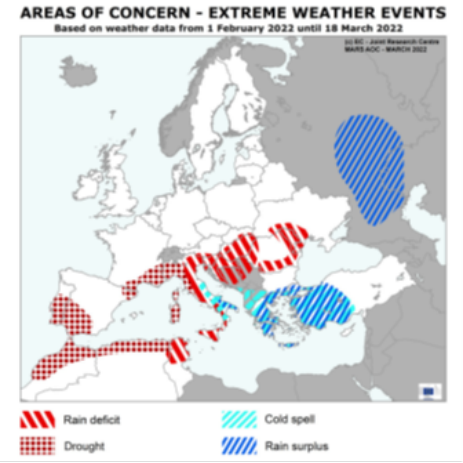

Figure S7: Areas of concern - Extreme weather events for February-March 2022. Extracted from Ben Aoun et al. (2022).

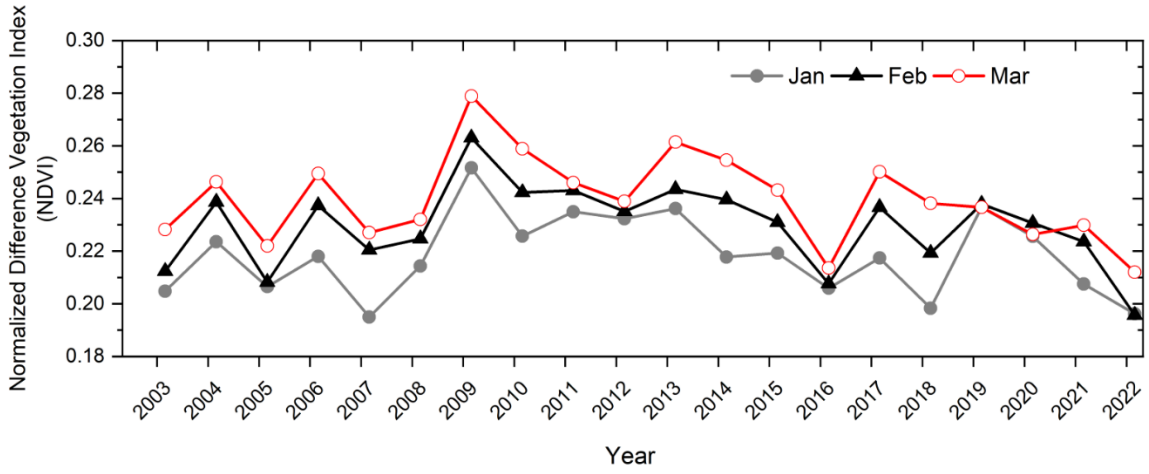

Figure S8: Monthly average values of the Normalized Difference Vegetation Index (NDVI) from MODIS (see https://modis.gsfc.nasa.gov/data/dataprod/mod13.php; last connection 15 September 2023) over the northernmost strip of the Maghreb [32°N, 7°W / 36.5°N 10°E] for January, February, and March in the period 2003-2022. The area bounded by [32°N, 7°W / 36.5°N 10°E] corresponds approximately to the drought areas in Morocco and Algeria reported by Bassu et al. (2022) and Baruth at al. (2023).

S4. Three-case analysis of "extreme" dust events

In this section, we take a closer look at the most intense events identified in the 2003-2022 period and mentioned in the present analysis. The events analysed in detail occurred on 20-24 February 2017 (Section 4.1), 27-31 March 2021 (Section 4.2), and 15-31 March 2022 (Section 4.3). Those in 2021 and 2022 were also analysed in detail by different international institutions

(see Table S1) because the social media impact. The associated synoptic situation in each of the three cases are described using NCEP/NCAR (see Section 2). The temporal evolution of the geopotential height (Z, in m) at 500 hPa (Z500) for each one of the three "extreme" dust events in the whole period 2003-2022 are shown in Figure S9. Averaged Z anomalies (m) at 925, 500, 200 hPa for each of the same five dust events are shown in Figure S10. Additionally, the analysis of these particular cases includes in-situ PM10 observations from European Environment Agency's air quality database (AirBase; https://www.eea.europa.eu/data-and-maps/data/aqereporting-9, last access 12 February 2024), satellite qualitative aerosol products based on the EUMESAT RGB dust (MetOffice; EUMETSAT, 2022) and daily dust forecasts based on MONARCH (Pérez et al, 2011; Klose et al,, 2021; https://dust.aemet.es/about-us/monarch, last access 12 February 2024) which is the reference operational forecast system at the WMO Barcelona Dust Regional Center (https://dust.aemet.es/about-us/wmo-dust-operations, 12 February 2024).

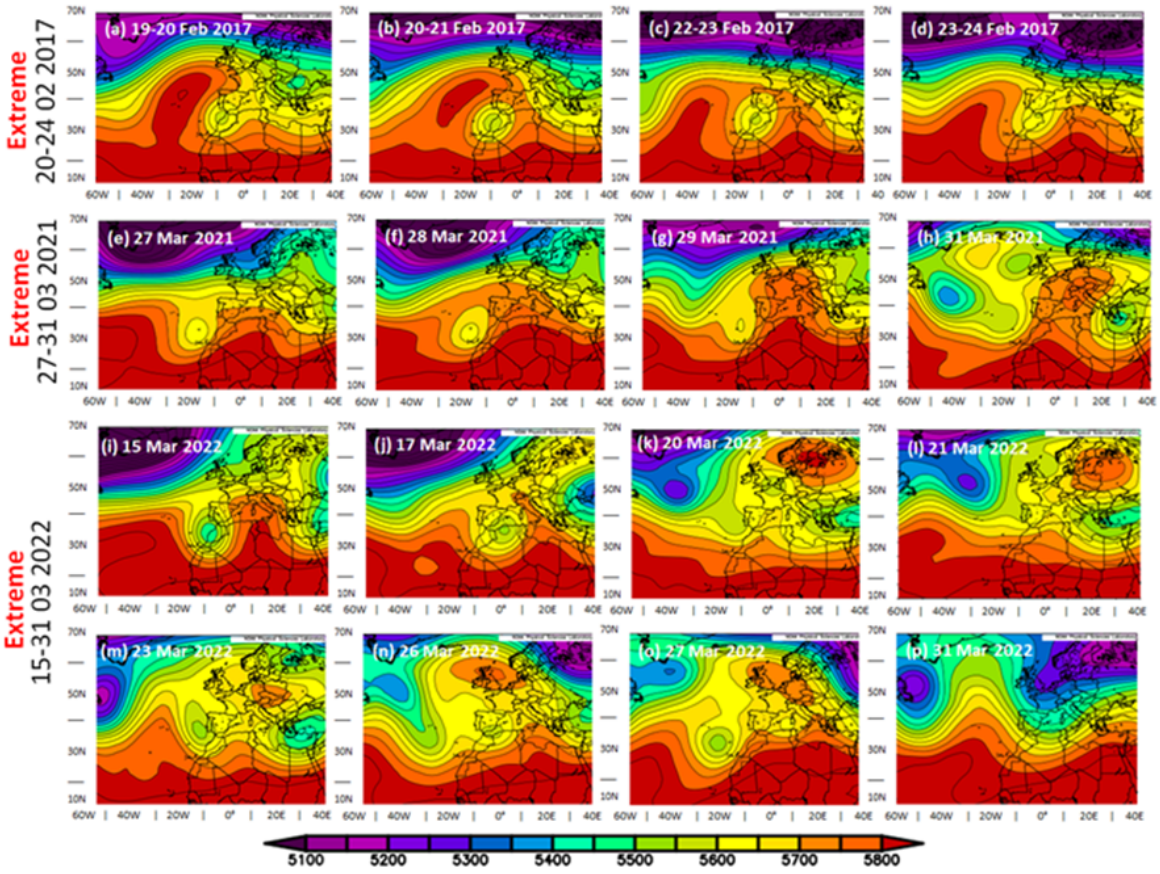

Figure S9: Averaged geopotential height fields (Z) at 500 hPa for sub-periods of time of the three strongest dust events (labelled as "extreme") occurred in the WEM on Feb. 20-24, 2017 ((a), (b), (c) and (d)); Mar. 27-31, 2021 ((e), (f), (g) and (h)); and Mar. 15-31, 2022 ((i), (j), (k), (l), (m), (n), (o), and (p)). Geopotential height fields have been obtained from NCEP/NCAR reanalysis.

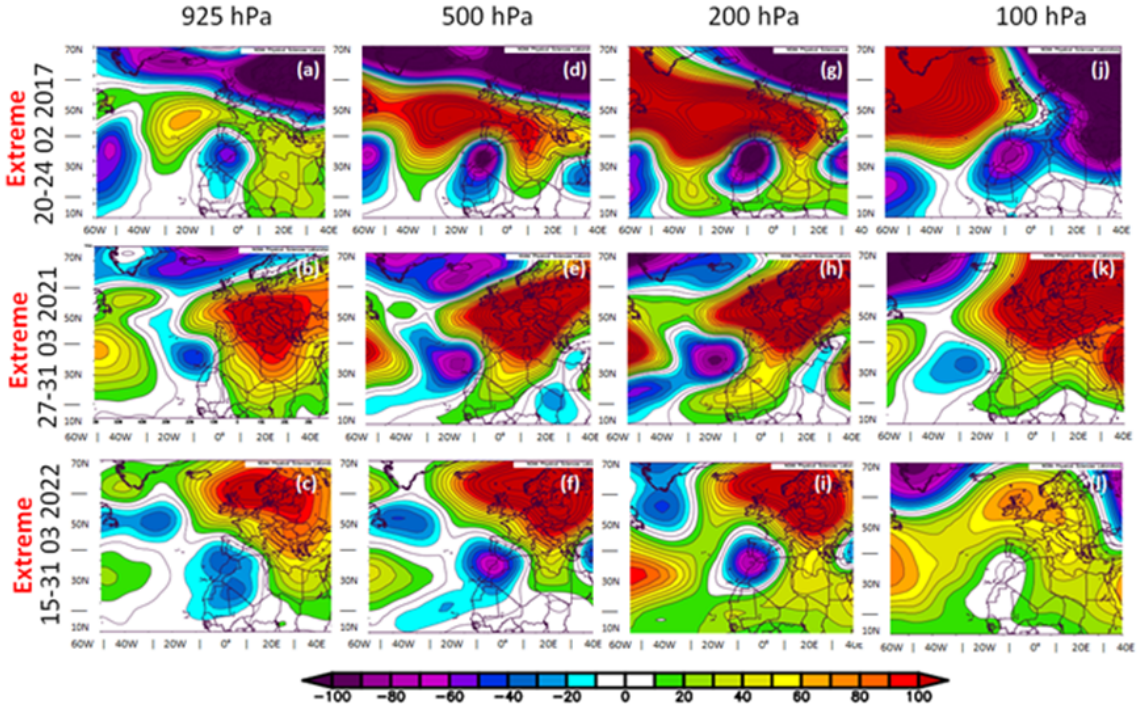

Figure S10: Geopotential height (Z) anomalies (m) at 925 hPa ((a), (b) and (c)), 500 hPa ((d), (e) and (f)), 200 hPa ((g), (h) and (i)), and 100 hPa ((j), (k) and (l)), with respect to the reference period 1991-2020, for the three strongest dust events (labelled as "extreme") occurred in the WEM on the following dates: Feb. 20-24, 2017; Mar. 27-31, 2021; and Mar. 15-31, 2022. Geopotential height fields have been obtained from NCEP/NCAR reanalysis.

S4.1. Case analysis #1: February 20-24, 2017

Fernandez et al. (2019) attributed this dust episode to a Sharaz cyclone, only reporting low-level geopotential height analyses (i.e. 850 hPa). They focused their study to properties of aerosols, qualifying this episode, as "an unprecedented extreme Saharan dust event" that mainly affected the Iberian Peninsula where AOD > 2 were measured by several sun-photometers of the AERONET network (Holben et al., 1998; Giles et al., 2019). This 5-day dust event yielded median and mean AOD values of 0.31 and 0.41, respectively, in our study region.

According to our analysis, the dust intrusion over Europe was caused by a cut-off low detached from the general circulation due to the interaction with a long and strong ridge over the North Atlantic (Figure S9 (a), (b), (c), and (d)). It is noteworthy that the Z anomalies for of each day of the event (not shown here) and those averaged over the 5 days that the event lasted are very similar throughout the troposphere, from near ground level (925 hPa; Figure S10 (a)) to the lower stratosphere (100 hPa; Figure S10 (j)), registering negative values < -100 m between 500 and 200 hPa where the cut-off low is found, and on the contrary, positive values, > +100 m, in a large strip that extends from the mid-latitude North Atlantic to central Europe, forming a persistent dipole-like pattern configuration. The cut-off low was initially centred on the NW of Morocco on February 20 (Figure S9 (a)) with slow retrograde movement towards the SW that caused dust rise from the mountainous areas of the NW of Algeria, specifically at Chott ech Chergui according with the sources identified by Ginoux et al. (2012), as seen from the RGB-SEVIRI animation (Figure S1 and Timelapse#1 at https://repositorio.aemet.es/handle/20.500.11765/15054), which produced a light dust plume towards the south of the Iberian Peninsula that can be identified with pink colour. Later, on February 21 dust was uplift from the interior of Algeria, producing a denser dust plume (stronger pink colour) towards the Mediterranean. On the 22nd, dust sources between NE Morocco and NW Algeria (Chott ech Chergui and Morocco Coastal

plains, according with the sources identified by Ginoux et al., 2012) activated significantly increasing dust amount transported to the south of the Iberian Peninsula. In its final phase, the low was absorbed by the mid-latitude circulation.

A year earlier, almost on the same dates (February 18-22, 2016), a shorter but similar dust intrusion took place, which has been labelled as "moderate" in this study. This dust event was subject of a detailed analysis by Oduber et al. (2019), which described this event as "unusual". They explained this dust intrusion by the combined effect of an Azores high very extended towards the East, and a low in North Africa, showing only the analysis of surface isobars. The authors didn't realize either that the real cause of this dust intrusion was a stationary cut-off low centred on the Atlantic coast of Morocco.

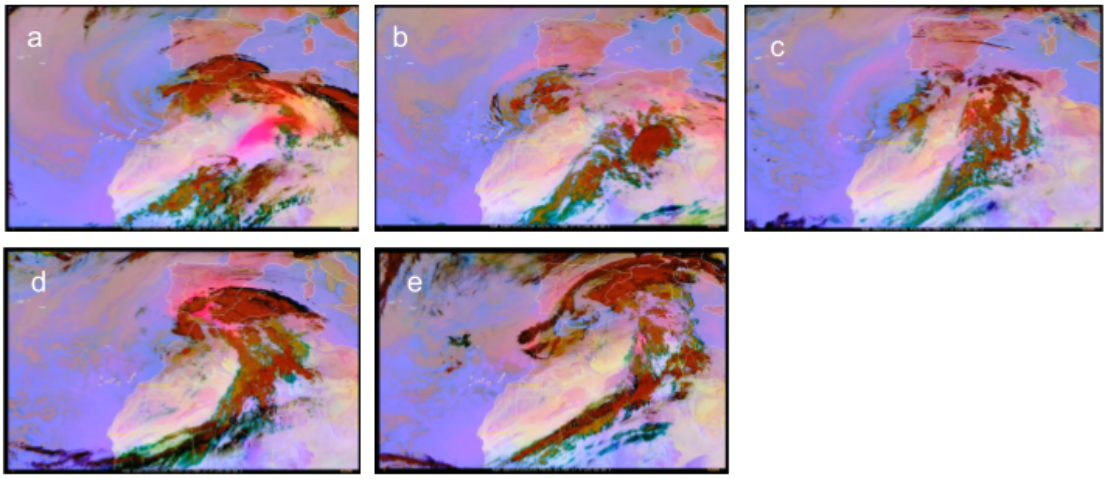

Figure S11: RGB dust product from MSG/SEVIRI at 0UTC for (a) 20 February 2017, (b) 21 February 2017, (c) 22 February 2017, (d) 24 February 2017, and (e) 24 February 2017. Dust is associated to pink colour.

S4.2 Case analysis #2: March 27-31, 2021

On March 27, 2021, began a 5-day dust event with AOD median and mean AOD values of 0.39 and 0.41, respectively, values, so being labelled as "extreme", the second chronologically of this category in the series of dust events since 2003. An isolated cut-off low centred over Madeira, combined with a strong ridge over the Western Mediterranean and France (Figure S9 (e)), favoured dust transport from Morocco and Mauritania to SW Iberian. At the end of this long dust event an Omega block centred on Western Europe on the 29th was established (Figure S9 (g)). An intense dust lift is then produced at the lee of the Atlas Mountains (south Morocco), a dust hot-point (Schepanski et al., 2012; Fiedler et al., 2014), generating a very dense dust plume that moved northwards crossing the entire west half of the Iberian Peninsula until the North Atlantic impacting the south of British Islands and, later, Belgium (Figure S12 and Timelapse#2 at https://repositorio.aemet.es/handle/20.500.11765/15054). Again, during this event, a dipole-like pattern of Z anomalies, with positive anomalies over Western Europe and negative anomalies from the persistent cut-off low, like those of previous cases, is well observed in the whole troposphere (Figure S10 (b), (e), (h), and (k)).

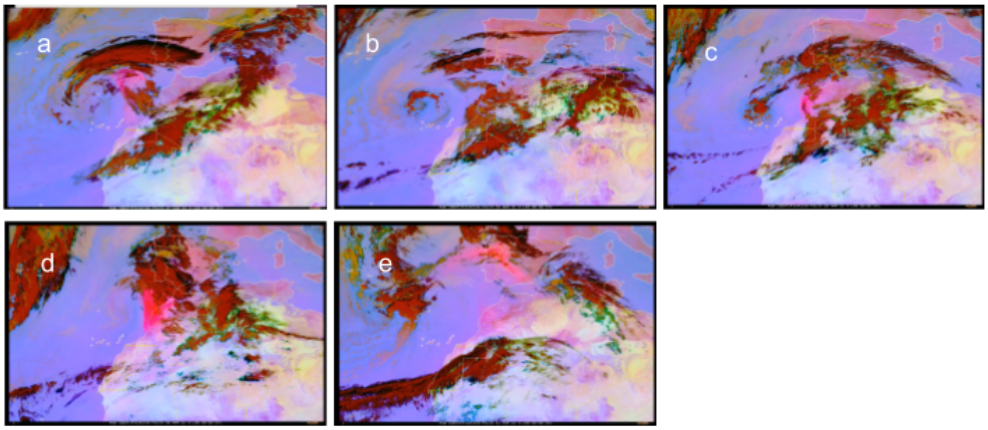

Figure S12: RGB dust product from MSG/SEVIRI at 0UTC for (a) 27 March 2021, (b) 28 March 2021, (c) 29 March 2021, (d) 30 March 2021, and (e) 31 March 2021. Dust is associated to pink colour.

S4.3 Case analysis #3: March 15-30, 2022

The very long-lasting (14 days) dust event of March 2022 (see Figure S13 and Timelapse#3 at https://repositorio.aemet.es/handle/20.500.11765/1505), with an AOD median and mean AOD values of 0.34 and 0.40, respectively, constitutes a milestone in the dust transport from North Africa to the WEM, impacting air quality of western Europe with rather high PM10 values (Figure S14). This event has broken all records, not only for duration and intensity but also for the huge area affected. This long dust event was due to the concatenation of four cut-off lows forced to move between the Canary Islands and the Iberian Peninsula by a persistent anticyclonic blocking over Western Europe (see the sequence of eight plots in Figure S9 (i), (j), (k), (l), (m), (n), (o), and (p)). This long dust event was initiated by the slow movement of the storm named Celia (cut-off low #1) over the North African coast from 14 to 16 March (see Figure S9 (a) and (b)). Celia began to lose intensity in the second half of the 15th and ceased to be named as such on the synoptic maps, although it (cut-off low #1) continued a gradual transition towards the Mediterranean region over through the north of the African continent (see the movement of Celia/cut-off low #1 in Figure S9 (i) and (j)), which remained isolated from the general circulation. Cut-off low #1, with forcing on its SE flank, produced a dense plume of dust that, at times, was difficult to identify among abundant cloudiness, which moved from the interior of Algeria towards the N-NW of the Iberian Peninsula reaching the North Atlantic and impacting France (see Figure S13 and Timelapse#3 at https://repositorio.aemet.es/handle/20.500.11765/15054). The dust plume that reached southwestern France on the early 15th was already at 50ºN 12 hours later, curving then to the East and moving at higher altitude, impacting central Europe (Figure S15 (a)) (cross section March 15 at 12 UTC). On the 16th at 3 UTC a second branch of the same dust plume curved to the southwest, returning to the African continent along the NW coast of Morocco (Figure S15 (b)) (March 16 at 03 UTC). Cut-off low #1 severely impacted the Iberian Peninsula, as can be seen by comparing the map of PM10 concentrations in Europe on March 13 (before the dust intrusion), in which most of the stations of the Iberian Peninsula and the Balearic Islands show concentrations of PM10 $\leq$ 20 $\mu g \cdot m^{-3}$ and that of March 15 in which many of these stations recorded concentrations of PM10 > 150 $\mu g \cdot m^{-3}$ (Figure S14 (a), (b)). The dust advection on the Peninsula subsided as of the second half of the 16th. However, cut-off low #1 continued advecting dust over the western Mediterranean from dust sources near the Algerian coast (Chott Melhir, Chott el Hodma, and Chott ech Chergui, dust sources identified by Ginoux et al. (2012)) until the arrival of a second deep low (cut-off low#2). The strong convection of the cut-off low#1 on 14-16 March was responsible for the significant thickness of the dust layer and the high level of dust transport (~ 5000 m height) impacting the Pyrenees and the Alps (Figure S15 (b)) (cross section March 16 at 3 UTC). Cut-off low #2 was centred on the 20th (Figure S9 (k)) over the coast of Morocco but remained stationary without advancing further to East, generating limited dust transport over the Mediterranean. Cut-off

low #3 on the 23rd (Figure S9 (m)) followed similar evolution to the first one, but without penetrating its circulation so much in the continent in such a way that it raised mineral dust from plateau areas of the Algerian Atlas being only advected to the south of the Iberian Peninsula (Figure S10 (c)), while cut-off low#3 weakened and moved to the Mediterranean. Finally, from 27th, the last deep low (cut-off low #4), more extensive, came down very close to the Canary Islands and in its shift to the E raised dust again from the NW of Algeria plateaus (Chott Melhir, Chott el Hodma, and Chott ech Chergu, according to Ginoux et al. (2012)), advecting dust to the western Mediterranean and impacting the Iberian Peninsula, the Balearic Islands, France, North Italy, Belgium, and western Germany increasing dramatically, again, the PM10 concentrations (PM10 > 50 $\mu g \cdot m^{-3}$) in many European air quality stations (see PM10 concentrations on Europe in March 29th; Figure S14 (d)). On the 30th, already in its final phase, cut-off low #4 produced new dust plumes from the river drainage basin of the Aïir around the Saharan mountain ranges in southern Algeria, moving towards the Central Mediterranean, while generating a huge dust front associated with a haboob in central Algeria. Meanwhile, the strong ridge over Europe continued until the last days of March, not so intense, and disappearing at the west of the British Islands. As in the four previous cases, a dipole-like pattern of Z anomalies is observed throughout the troposphere, with positive values covering a wide band over Europe and the North Atlantic, and negative anomalies in the region between the Canary Islands and the Iberian Peninsula (Figure S10 (c), (f), (i), and (l)). In this case, since it is a very long period, the train of three cut-off lows can be observed at 500 and 200 hPa (Figure S10 (f) and (i)).

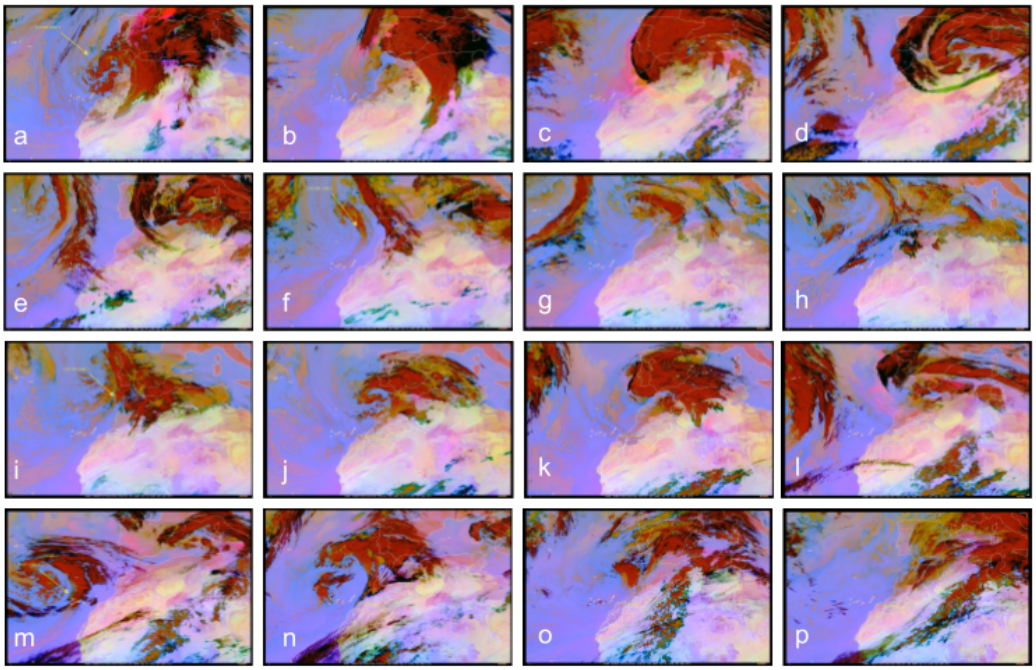

Figure S13: RGB dust product from MSG/SEVIRI at 3UTC for (a) 15 March 2022, (b) 16 March 2022, (c) 17 March 2022, (d) 18 March 2022, (e) 19 March 2022, (f) 20 March 2022, (g) 21 March 2022, (h) 22 March 2022, (i) 23 March 2022, (j) 24 March 2022, (k) 25 March 2022, (m) 26 March 2022, (n) 27 March 2022, (o) 28 March 2022 and (p) 29 March 2022. Dust is associated to pink colour.

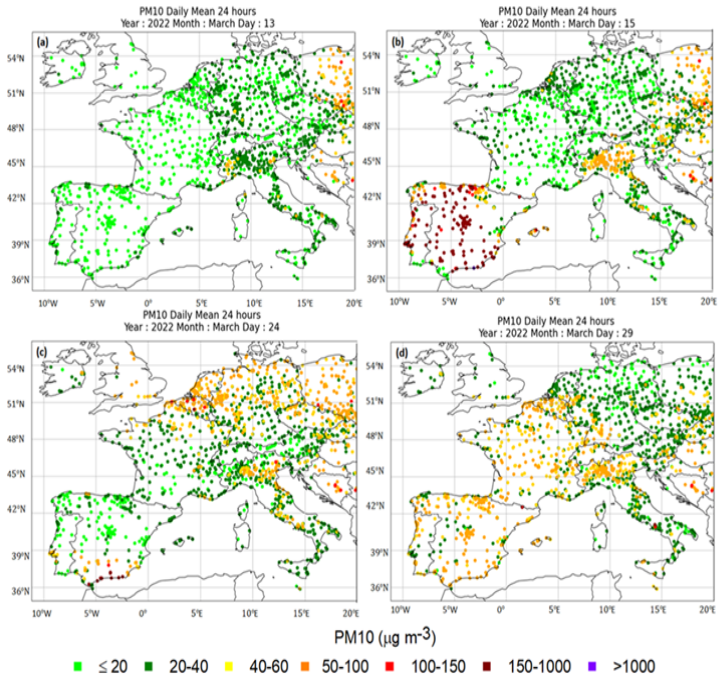

Figure S14: Daily mean PM10 (µg·m^{-3}) at the European stations on (a) 13 March 2022, (b) 15 March 2022, (c) 24 March 2022, and (d) 29 March 2022. Data from the European Environment Agency (EAA).

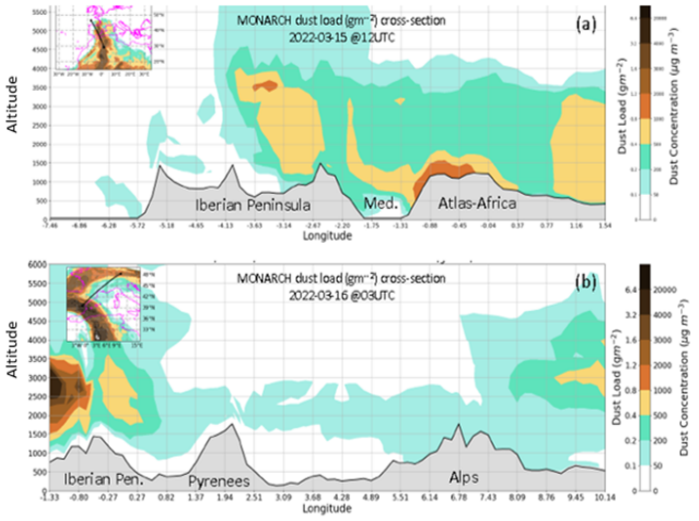

Figure S15: Forecasted vertical cross-sections and dust concentration (µg·m^{-3}) (dust load (g·m^{-2})) on (a) 15 March 2022 at 12 UTC and on (b) 16 March 2022 at 3 UTC. Dust forecast from MONARCH.

S5. Considerations on the ability of cut-off lows to mobilize and raise dust from the ground.

For the three case studies presented in Section S4, we have first identified the dust hotspots using the RGB dust animations and then doublechecked the surface wind speeds from the 6-hourly NCEP/NCAR reanalysis at 00, 06, 12 and 18 UTC are within the windspeed threshold range to activate dust sources given by Helgren and Prospero (1987). Figure S16 shows surface vector wind at 00, 06,12 and 18 UTC for March 27, 2021 (considered as “moderate” in the resulting analysis). Relatively large

regions covering dust hotspots over Morocco, Western Sahara, Mauritania or Algeria, show surface vector wind within the range of the wind speeds threshold (5.0-12.5 $m \cdot s^{-1}$) considered by Helgren and Prospero (1987).

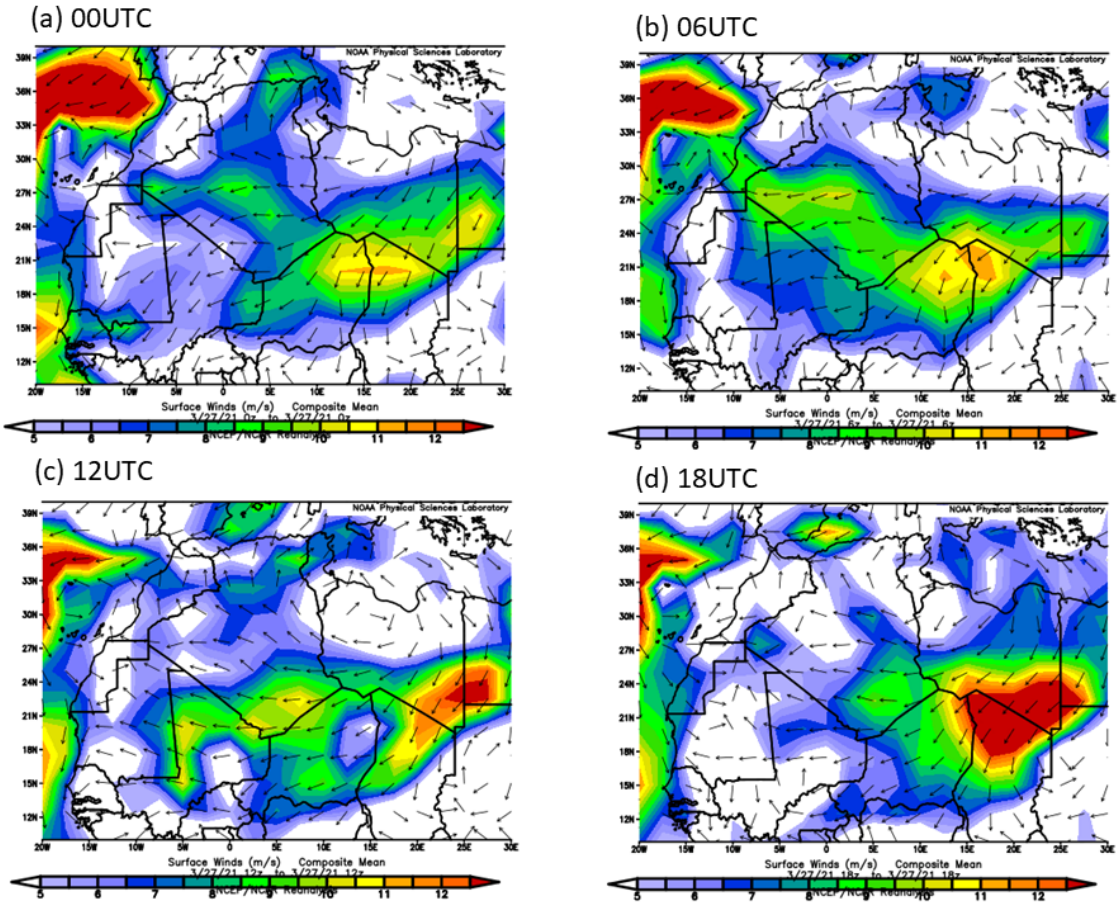

Figure S16: NCEP Reanalysis surface vector wind for March 27, 2021: (a) 0 UTC; (b) 6 UTC; (c) 12 UTC; and (d) 18 UTC; Wind speed scale ranges from 5 to 12.5 ms^{-1}.

S6. Blocking and jet stream frequency anomaly during dust days in western Euro-Mediterranean in February and March 2020-2022 period.

There are marked differences between February and March 2020-2022 (Figure S17). In February 2020-2022, blocking activity was almost suppressed over central Europe, and increased over the Mediterranean, resulting in intensification of the jet at mid-latitudes. March 2020-2022 was characterized by poleward jets and enhanced blocking over the climatological region of occurrence. These intra-seasonal contrasts weaken the signal and significance shown in Figure S17 of the main text for February-March.

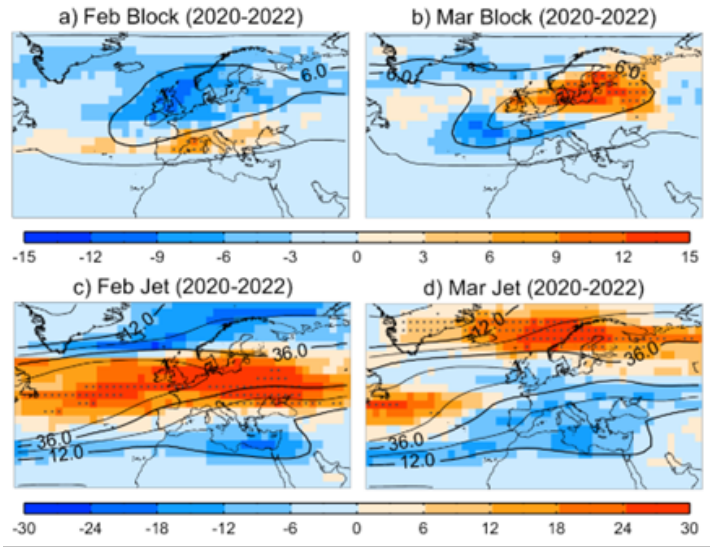

Figure S17: Blocking (a,b) and jet stream (c,d) frequency anomaly during dust days (in our study region) in February and March 2020-2022 period. Frequencies are expressed in percentage of dust days of the period and anomalies (colour shading) are defined with respect to the expected frequency of occurrence (contours). Dots denote significant positive anomalies at $p<0.05$ (i.e. grid points where local blocking and jet frequency is significantly higher than expected), as inferred from a 500-trial bootstrap. The expected frequency of occurrence is defined as the mean of the 500 random members, all with the same sample size as the number of considered days but random dates of occurrence. Geopotential height fields have been obtained from ERA5 reanalysis.

S7. Dust intrusions in winter 2022-2023

To assess whether the anomalous conditions of the 2020-2022 winters persisted during the winter of 2023 we have evaluated the available data for February and March 2023 (Figure S18). The 2022-2023 winter was characterised by a severe drought in the north of Morocco, Algeria, and the Iberian Peninsula (Tarnavsky et al., 2023). A 6-day strong dust event occurred on 18-23 February 2023 with mean AOD of 0.31± 0.09, and a maximum daily AOD of 0.41 on 21 February (Figure S19). Like for the dust events of the 2020-2022 period, dust uplift and its transport to the study region was associated with two concatenated cut-off lows in the vicinity of the Canary Islands. This dust event was also accompanied by positive Z500 anomalies over central Europe and the Mediterranean, like the patterns of low-latitude blocks and subtropical ridges. However, no dust event was recorded in March 2023, indicating that the unusually high frequency of western Mediterranean dust intrusions did not continue during the winter of 2023, which supports our choice of 2020-2022 as the anomalous period.

A preliminary analysis of dust intrusions in winter 2022-2023 can be summarised in Figures S18 and S19. The results show a peak in February 2023 associated to a particular event that affected the Iberian Peninsula. February 2023 is also observed a maximum in Sea Surface Temperature (SST) as it is shown in the time series of averaged region-monthly mean for each winter month (i.e., January, February and March) and the 2003-2023 period in the region that covers the easternmost part of the subtropical North Atlantic Ocean, and the westernmost Mediterranean (Alborán Sea and Balearic Islands) [30-40ºN, 15ºW-5º] is shown in Figure S20.

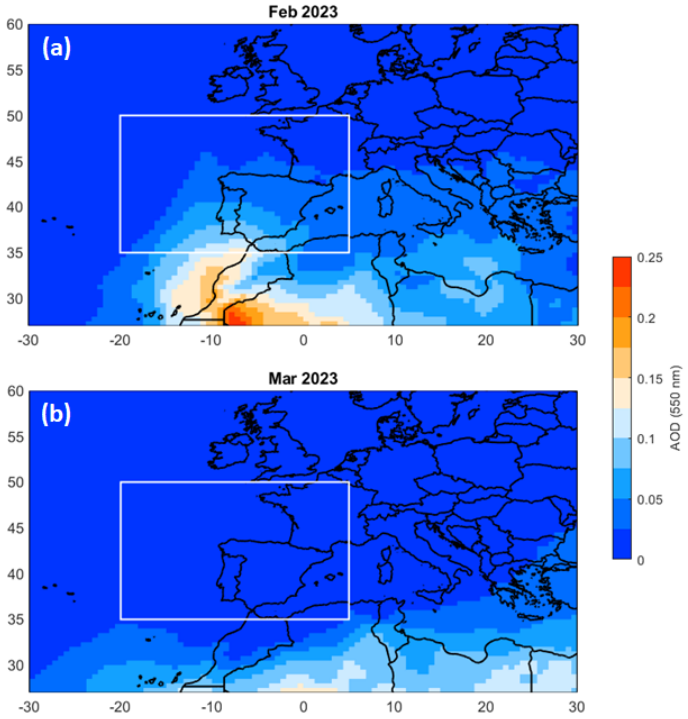

Figure S18: Averaged AOD-550 nm for (a) February 2023, and (b) March 2023. Rectangle with a white perimeter (35ºN-50ºN, 20ºW-5ºE) marks the WEM. Results based on MERRA-2 reanalysis.

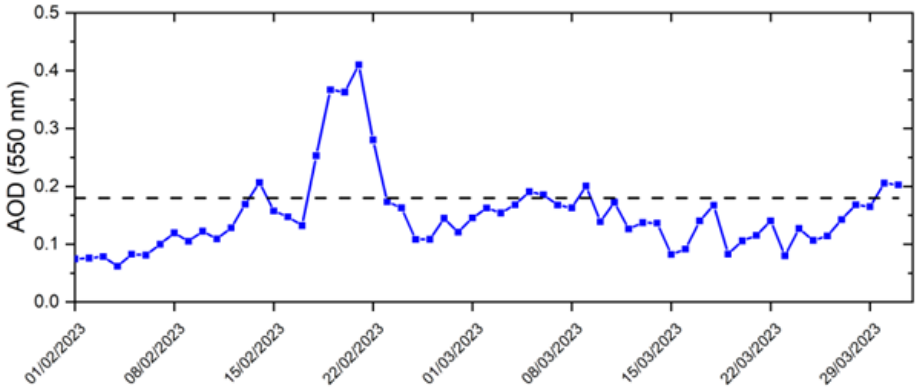

Figure S19: Daily averaged AOD within our study region [35-50ºN, 20ºW-5ºE], from February 1st to March 31, 2023. Results based on MODIS/Aqua AOD database.

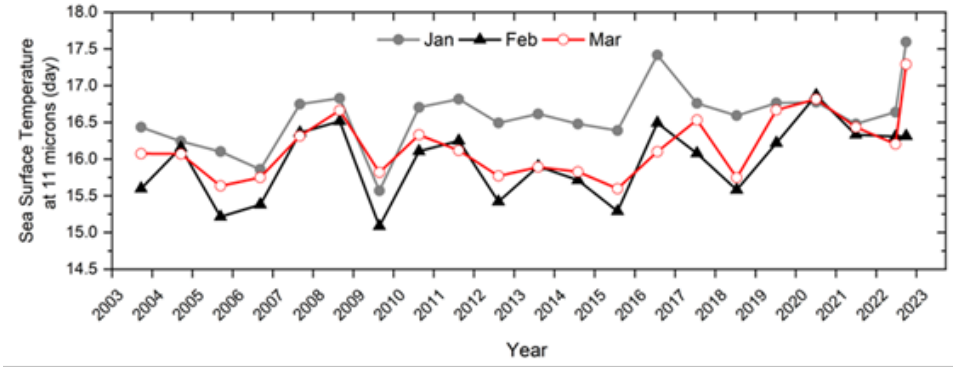

Figure S20: Time series of averaged region-monthly mean for each winter month (i.e., January, February and March) and the 2003-2023 period of the Sea Surface Temperature (SST) in the region that covers the easternmost part of the subtropical North Atlantic Ocean, and the westernmost Mediterranean (Alborán Sea and Balearic Islands) [30-40ºN, 15ºW-5º]. Results based on MODIS Water Reservoir Monthly L3 Global product (https://modis.gsfc.nasa.gov/data/dataprod/mod28.php).

References

Baruth, B., Bassu, S., Ben Aoun, W., Biavetti, I., Bratu, M., Bussay, A., Cerrani, I., Chemin, Y., Claverie, M., De Palma, P., Fumagalli, D., Manfron, G., Morel, J., Nisini, L., Panarello, L., Rossi, M., Seguini, L., Tarnavsky, E., Van Den Berg, M., Zajac, Z. and Zucchini, A., JRC MARS Bulletin - Crop monitoring in Europe - March 2023 - Vol. 31 No 3, Van Den Berg, M., Niemeyer, S. and Baruth, B. editor(s), Publications Office of the European Union, Luxembourg, https://dx.doi.org/10.2760/152370, JRC133043, 2023.

Bassu, S., Ben Aoun, W., Biavetti, I., Bratu, M., Cerrani, I., Chemin, Y., Claverie, M., De Palma, P., Fumagalli, D., Manfron, G., Morel, J., Nisini Scacchiafichi, L., Panarello, L., Ronchetti, G., Seguini, L., Toreti, A., Van Den Berg, M., Zajac, Z. and Zucchini, A.,: JRC MARS Bulletin - Crop monitoring in Europe - April 2022 , Vol. 30, No 4, Van Den Berg, M. and Belward, A. editor(s), Publications Office of the European Union, Luxembourg, doi:10.2760/556986, JRC127960, 2022.

Ben Aoun, W., Claverie, M., Chemin, Y., Seguini, L., Toreti, A., Manfron, G., Cerrani, I., Panarello, L., Baruth, B., Bassu, S., Biavetti, I., Fumagalli, D., Lecerf, R., Zajac, Z., Zucchini, A., Van Den Berg, M., Bratu, M., De Palma, P., Morel, J., Nisini Scacchiafichi, L., Niemeyer, S. and Ronchetti, G., JRC MARS Bulletin - Crop monitoring in Europe - March 2022 - Vol. 30 No 3, Van Den Berg, M., Van Der Velde, M. and Niemeyer, S. editor(s), Publications Office of the European Union, Luxembourg, https://dx.doi.org/10.2760/888247, JRC127959, 2022.

Buchard, V., Randles, C. A., da Silva, A. M., Darmenov, A., Colarco, P. R., Govindaraju, R., Ferrare, R., Hair, J., Beyersdorf, A. J., Ziemba, L. D., and Yu, H.: The MERRA-2 Aerosol Reanalysis, 1980 Onward. Part II: Evaluation and Case Studies, Journal of Climate, 30 17, 6851-6872, https://doi.org/10.1175/JCLI-D-16-0613.1, 2017.

Escribano, J., Di Tomaso, E., Jorba, O., Klose, M., Gonçalves Ageitos, M., Macchia, F., Amiridis, V., Baars, H., Marinou, E., Proestakis, E., Urbanneck, C., Althausen, D., Bühl, J., Mamouri, R.-E., and Pérez García-Pando, C.: Assimilating spaceborne lidar dust extinction can improve dust forecasts, Atmos. Chem. Phys., 22, 535–560, https://doi.org/10.5194/acp-22-535-2022, 2022.

Fernández, A.J., Sicard, M., Costa, M.J., Guerrero-Rascado, J.L., Gómez-Amo, J.L., Molero, F., Barragán, R., Basart, S. Bortoli, D., Bedoya-Velásquez, A.E., Utrillas, M.P., Salvador, P., Granados-Muñoz, M.J., Potes, M., Ortiz-Amezcua, P., Martínez-Lozano, J.A., Artíñano, B., Muñoz-Porcar, C., Salgado, R., Román, R., Rocadenbosch, F., Salgueiro, V., Benavent-Oltra, A., Rodríguez-Gómez, A., Alados-Arboledas, L., Comerón, A., Pujadas, M.: Extreme, wintertime Saharan dust intrusion in the Iberian Peninsula: Lidar monitoring and evaluation of dust forecast models during the February 2017 event, Atmospheric Research, 228, 223-241, ISSN 0169-8095, https://doi.org/10.1016/j.atmosres.2019.06.007, 2019.

Fiedler, S., Schepanski, K., Knippertz, P., Heinold, B., and Tegen, I.: How important are atmospheric depressions and mobile cyclones for emitting mineral dust aerosol in North Africa?, Atmos. Chem. Phys., 14, 8983–9000, https://doi.org/10.5194/acp-14-8983-2014, 2014.

Giles, D. M., Sinyuk, A., Sorokin, M. G., Schafer, J. S., Smirnov, A., Slutsker, I., Eck, T. F., Holben, B. N., Lewis, J. R., Campbell, J. R.,Welton, E. J., Korkin, S. V., and Lyapustin, A. I.: Advancements in the Aerosol Robotic Network (AERONET) Version 3 database – automated near-real-time quality control algorithm with improved cloud screening for Sun photometer aerosol optical depth (AOD) measurements, Atmos. Meas. Tech., 12, 169–209, https://doi.org/10.5194/amt-12-169-2019, 2019.

Ginoux, P.. Prospero, J. M., Gill, T. E., Hsu, N. C., and Zhao, M.: Global-scale attribution of anthropogenic and natural dust sources and their emission rates based on MODIS Deep Blue aerosol products, Rev. Geophys., 50, RG3005, https://doi.org/10.1029/2012RG000388, 2012.

Helgren, D. M., and Prospero, J. M.: Wind Velocities Associated with Dust Deflation Events in the Western Sahara, Journal of Climate and Applied Meteorology, 26, 9, 1147–1151. https://www.jstor.org/stable/26183511, 1987.

Holben, B., Eck, T., Slutsker, I., Tanré, D., Buis, J., Setzer, A., Vermote, E., Reagan, J., Kaufman, Y., Nakajima, T., Lavenu, F., Jankowiak, I., and Smirnov, A.: AERONET–A Federated Instrument Network and Data Archive for Aerosol characterization, Remote sensing environment, 66, 9, 1147-1151, https://doi.org/10.1016/S0034-4257(98)00031-5, 1998

Kleist, D. T., Parrish, D.F.,Derber, J.C., Treadon, R., Wu, W.-S., and Lord, S.: Introduction of the GSI into the NCEP Global Data Assimilation System, Wea. Forecasting, 24, 1691–1705, doi:10.1175/2009WAF2222201.1, 2009.

Klose, M., Jorba, O., Gonçalves Ageitos, M., Escribano, J., Dawson, M. L., Obiso, V., Di Tomaso, E., Basart, S., Montané Pinto, G., Macchia, F., Ginoux, P., Guerschman, J., Prigent, C., Huang, Y., Kok, J. F., Miller, R. L., and Pérez García-Pando, C.: Mineral dust cycle in the Multiscale Online Nonhydrostatic AtmospheRe CHemistry model (MONARCH) Version 2.0, Geosci. Model Dev., 14, 6403–6444, https://doi.org/10.5194/gmd-14-6403-2021, 2021.

Met Office; EUMETSAT (2022): MSG: Dust imagery in the RGB channels over the full disc at 41.5 degrees East (LEDF41, up to 0900 UTC 1st June 2022). NERC EDS Centre for Environmental Data Analysis, date of citation. https://catalogue.ceda.ac.uk/uuid/b1dacc09b42f4d8ab492c5d5c751efa9.

Molod, A. M., Takas, L.L., Suarez, M., and Bacmeister, J.: Development of the GEOS-5 atmospheric general circulation model: Evolution from MERRA to MERRA-2, Geosci. Model Dev., 8, 1339–1356, doi:10.5194/gmd-8-1339-2015, 2015.

Oduber, F., Calvo, A.I., Blanco-Alegre, C., Castro, A., Nunes, T., Alves, C., Sorribas, M., Fernández-González, D,. Vega-Maray, A.M., Valencia-Barrera, R.M., Lucarelli, F., Nava, S., Calzolai, G., Alonso-Blanco, E., Fraile, B., Fialho, P., Coz, E., Prevot, A.S.H., Pont, V., Fraile, R.: Unusual winter Saharan dust intrusions at Northwest Spain: Air quality, radiative and health impacts, Sci. Total Environ.;669,213-228, doi: 10.1016/j.scitotenv.2019.02.305, 2019.

Pérez, C., Haustein, K., Janjic, Z., Jorba, O., Huneeus, N., Baldasano, J. M., Black, T., Basart, S., Nickovic, S., Miller, R. L., Perlwitz, J. P., Schulz, M., and Thomson, M.: Atmospheric dust modeling from meso to global scales with the online NMMB/BSC-Dust model – Part 1: Model description, annual simulations and evaluation, Atmos. Chem. Phys., 11, 13001–13027, https://doi.org/10.5194/acp-11-13001-2011, 2011.

Schepanski, K., Tegen, I., and Macke, A.: Comparison of satellite based observations of Saharan dust source areas, Remote Sensing of Environment, 123, 012, 90-97, ISSN 0034-4257, https://doi.org/10.1016/j.rse.2012.03.019, 2012.

Tarnavsky, E., Rossi, M., Bussay, A., Morel, J., Biavetti, I., Bratu, M., Cerrani, I., Claverie, M., De Palma, P., Fumagalli, D., Manfron, G., Niemeyer, S., Nisini, L., Panarello, L., Van Den Berg, M. and Zucchini, A., JRC MARS Bulletin - Crop monitoring in Europe - December 2023 - Vol. 31 No 12, Van Den Berg, M. editor(s), Publications Office of the European Union, Luxembourg, 2023, doi:10.2760/197325, JRC133192.